Asian Journal of Chemistry; Vol. 36, No. 7 (2024), 1601-1608

ASIAN JOURNAL OF CHEMISTRY

https://doi.org/10.14233/ajchem.2024.31757

Theoretical, Antibacterial and Antioxidant Investigations of Hydroxyl Group Substituted Benzanilide Schiff Bases

G.K. AYYADURAI[1,], S. RATHIKA[2,], S. SUMATHI[2,] and R. JAYAPRAKASH[3,*,]

[1]Department of Chemistry, Sri Sairam Engineering College, Sai Leo Nagar, West Tambaram, Chennai-600044, India
[2]Department of Chemistry, Sri Sairam Institute of Technology, Sai Leo Nagar, West Tambaram, Chennai-600044, India
[3]Department of Chemistry, School of Arts and Science, Vinayaka Mission's Chennai Campus, Vinayaka Mission's Research Foundation (Deemed University), Paiyanoor, Chennai-603104, India

*Corresponding author: E-mail: jayaprakashsangee1977@gmail.com

Received: 17 April 2024; *Accepted*: 20 May 2024; *Published online*: 29 June 2024; AJC-21680

Two novel Schiff bases were synthesized from 4-amino-N-(4-aminophenyl)benzamide (DABA) and investigated after the spectral characterization techniques. Density functional theory (DFT) and molecular docking studies were conducted initially for the molecules for drug suitability. The toxicity of the synthesized molecules was evaluated using brine shrimp and 50% mortality concentrations of both the Schiff bases were examined with standard vincristine sulphate. Then, the antimicrobial activity was studied against selected bacterial strains such as *E. coli*, *K. pneumoniae*, *S. typhimurium* and *P. mirabilis*. The biological efficacy also extended to antioxidant study and the results showed that the inhibition concentrations between 150 and 305 µg/mL, which are in the toxicity limit. Out of two molecules, 2,4-dihydroxy group substituted Schiff bases showed better antimicrobial, antidiabetic and antioxidant activities.

Keywords: Benzanilide Schiff bases, DFT, Docking, Biological efficacy.

INTRODUCTION

In medicine, organic substances with a secondary amide group is used frequently. Rhodamine, meropenem, cephalexin, aztre-onam, docarpamine, ampicillin, gentamycin and ritonavir are some other examples [1,2]. The amide group has shown a wide range of biological activities, such as anti-inflammatory and antiangiogenic effects [3]. It is also used as a building block to make many therapeutic chemicals. Schiff bases are used a lot in the medicinal and medical fields because they have many biological effects, such as pain relief, anti-inflammatory, anti-bacterial, antitubercular, anticancer, antioxidant, *etc*. [4,5].

The nitrogen atom in azomethine disrupts normal cellular processes and potentially forms hydrogen bonds with the active centers of several cellular components. So, in order to make effective Schiff bases, this study chose the secondary amide group, which is made up of aromatic molecules, hydroxyl groups and azomethine groups. As more stable and non-carcinogenic colorants, *o*-vanillin and 2,4-dihydroxy benzaldehydes were used in the synthesis [6-8]. It was possible to make a large number of polymers, dyes, azetidinones and thiazolidinones from Schiff bases by using 4,4′-diamino benzanilide (DABA) [9]. DABA has many other uses, such as killing insects and stopping the growth of tuberculosis. However, the recognition of DABA Schiff base derivatives, their biological mechanisms, spectral analysis, and the application of docking and density-functional theory (DFT) in their study is still limited. In this study, two DABA based Schiff bases were synthesized by reacting *o*-vanillin and 2,4-dihydroxy benzaldehyde in methanol and characterized with UV, fluorescence, FT-IR and ^{1}H NMR spectra. The Spartan-14 software was used to compare the spectra with the theoretical density functional theory (DFT) data, except for the fluorescence spectra [10,11]. In addition, The microbial activities of the synthesized two Schiff bases and their *in vitro* antioxidant activities were also investigated. It was anticipated that these two pharmacologically potent compounds, if they contain a secondary amide group, will create new chemical structures that are likely to have unique biological features.

EXPERIMENTAL

Most of the chemicals were acquired from SRL chemicals, India and used without any further purification. The other compounds, *viz*. 4,4′-diaminobenzanilide (DABA, TCI chemicals, India) and aldehyde derivatives were procured from E. Merck, USA. To monitor the progress of chemical reactions, the TLC plates containing a hexane-ethyl acetate solvent mixture in a ratio of 60:40. A Sunsim electric melting point apparatus was used to measure the melting points. The UV and fluorescence spectrum were recorded by using Perkin-Elmer LS25 and LS45 instruments, respectively. The Jasco-6300 spectrometer was used to obain the vibrational spectra. The ^{1}H NMR spectra were recorded on a Bruker NMR400 spectrometer in DMSO solvent and the mass spectrum was recorded by Shimadzu LC-MS 2020 (Shimadzu, Japan).

Computational details: The experimental FT-IR spectra were interpreted using IRPal-2 software, whereas Spartan-14 DFT software was used to calculate of theoretical UV, FT-IR, proton and carbon NMR. The density functional theoretical computations of the synthesized DABA Schiff bases were accomplished using Spartan-14 Hartree-Fock, PM3 and 3-21G basis set to derive the complete geometry optimization. The optimization of the geometry, which corresponds to a real minimum, was achieved by letting all the parameters relax and ensuring that no imaginary frequencies were included in the calculations. Further, the frontier orbital (HOMO–LUMO) analysis, MEP analysis and potential map were also performed using the same method. The program was run in I-3 processor, 2GB RAM Dell system. Docking affinity score was calculated using online mcule 1-click docking server and the downloaded best pose was used for offline CLC drug discovery work bench-3 docking.

Biological materials: Artemia cyst eggs were purchased from fish shops and hatched in collected sea water from Besant Nagar, Chennai, India. Bacterial strains were purchased from the American type culture collection; *Escherichia coli* (ATCC 25922), *Klebsiella pneumoniae* (ATCC 35657), *Salmonella typhimurium* (ATCC 14028) and *Proteus mirabilis* (ATCC 35659). The DPPH free radical scavenging assay was used to investigate the antioxidant activity.

Synthesis of DABA based Schiff bases: Schiff bases **I** and **II** were synthesized by treating 0.1 mmol of 4,4′-diamino benzanilide (DABA) dissolved in 50 mL of ethanol with the ethanolic solution of 0.2 mmol of respective aldehydes. After 30 min of stirring at room temperature, the reaction mixture was gradually heated to reflux in water bath for 120 min. The progress of the reaction, TLC was employed using a 30:70 ethanol-hexane solvent solution. The obtained crude yellow (**I**)/light orange (**II**) solid was filtered after 2 h of cooling to room temperature and washed with 50 mL of hot ethanol (**Scheme-I**). Then, an equal ratio of ethanol and DMF was used for the recrystallization and the solid was dried in a vacuum oven at 70 ºC.

Characterization: The electronic absorption spectra of Schiff bases **I** and **II** in DMSO were recorded and both Schiff bases have exposed absorption band between 200 nm and 350 nm in the UV region. The synthesized Schiff bases were dissolved in DMSO solvent and their absorption spectra were recorded in the spectral range from 230 nm to 600 nm. Similarly, the fluorescence of Schiff bases was studied between 400 to 900 nm in DMSO solvent. The FT-IR spectra of Schiff bases **I** and **II** were recorded in the region 4000-400 cm^{-1} using Jasco-6300 spectrophotometer by KBr pellet technique. ^{1}H NMR spectra was recorded at room temperature on a Bruker NMR at 400 MHz spectrometer in DMSO solvent.

HF/DFT studies: Spartan-14 parallel 64-bit version (Wave function Inc., USA) quantum chemical package was used within the framework of DFT. The synthesized Schiff base **I** and **II** structures were drawn in Spartan-14 and using Hartree-

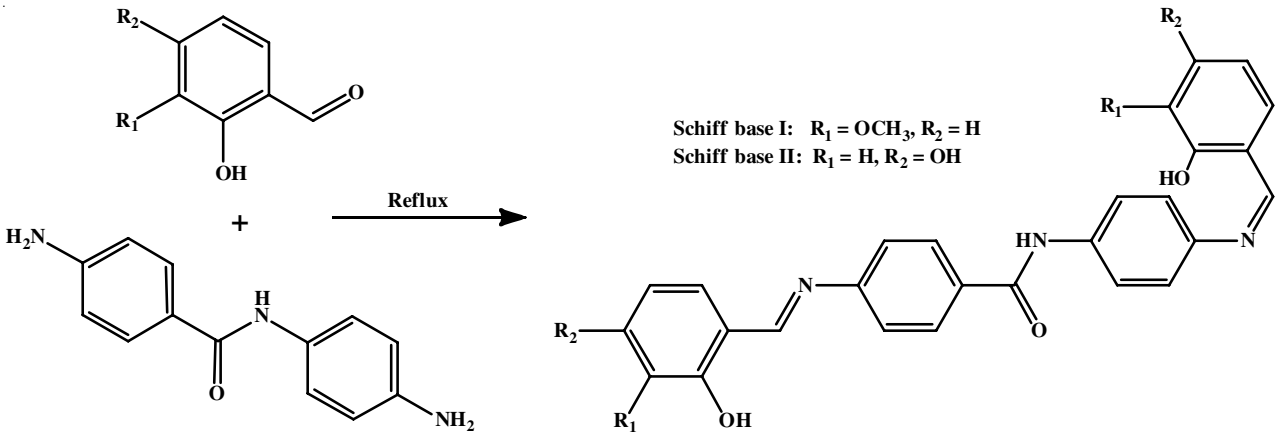

4-(((*E*)-2-Hydroxy-3-methoxybenzylidene)amino)-*N*-(4-(((*Z*)-2-hydroxy-3-methoxybenzylidene)amino)phenyl)benzamide (Schiff base I)
4-(((*E*)-2,4-Dihydroxybenzylidene)amino)-*N*-(4-(((*Z*)-2,4-dihydroxybenzylidene)amino)phenyl)benzamide (Schiff base II)

Schiff base	Yield (%)	Colour	m.p. (°C)	Solubility
I	85	Orange	250	DMSO/DMF
II	89	Yellow	>360	DMSO/DMF

Scheme-I: Preparation procedures of DABA Schiff bases **I** and **II**

Fock/B3LYP setup quantitative structure activity relationship (QSAR) parameters such as HOMO-LUMO gap, molecular electrostatic potential map and the chemical reactivity of the molecular structures. From the energies of Frontier molecular orbitals (FMO) energy band gap molecular properties like electronegativity (χ), chemical potential (μ), global hardness (η), global softness (S) and global electrophilicity index (ω) were calculated using the following formulas [12]:

Electronegativity:

$$\chi = -\frac{(E_{HOMO} + E_{LUMO})}{2}$$

Global hardness:

$$\eta = \frac{(E_{LUMO} - E_{HOMO})}{2}$$

Chemical potential:

$$\mu = -\chi$$

Global softness:

$$S = 0.5\ \eta$$

Softness:

$$\sigma = \frac{1}{\eta}$$

Global electrophilicity index:

$$\omega = \frac{0.5\mu^2}{\eta}$$

Docking studies: The binding sites and affinities of the synthesized Schiff bases were estimated using *in silico* modelling approaches [13,14]. Synthesized Schiff bases structures drawn in Chemdraw ultra were translated to smiles notation and docked against biologically relevant protein targets in online mcule-1 click docking station. The server calculated the docking score for Zipa (PDB ID-1s1j, Binding site: X- 26.0168, Y- 14.1613 and Z – 3.9038), dehydrosqualene synthase (PDB ID-2zcq, Binding site: X-17.5902, Y- 52.3671, Z-38.0749), m-RNA-capping enzyme subunit alpha (PDB ID-1p16, Binding site: X-4.3091, Y- 104.04, Z-71.5702), α-amylase (PDB ID-1xcw, Binding site: X- 7.5056, Y- 16.4744, Z – 42.5543) and breast cancer type 1 susceptibility protein (PDB ID-3k0k, Binding site: X- -23.4849, Y- 56.5041 and Z – 2.4167) targets. The obtained online docking scores of the submitted ligands, highest docking score pose was imported to CLC workbench-3 software and was verified the online values. The docking scores of the synthesized ligands at the specified binding site (exact amino acid) of proteins within the radius of 13 Å were calculated using the same drug discovery package. CLC drug discovery work bench-3 software was used to perform docking at selected common active amino acids (glutamine, aspartame) target site and then the docking scores were calculated for the studied molecules.

Artemia salina toxicity assay: Based on the docking results, brine shrimp lethal assay (BSLA) was used to calculate the lethal concentration for 50% (LC_{50}) mortality of the derived Schiff bases by regression graph method [15]. The natural sea water was mixed with one capsule of Artemia cyst eggs and maintained under aeration for 1 L. The beaker was exposed to a 60 W tungsten light for 30 h. After the completion of the hatching process, brine shrimp larvae were taken for toxicity study. Test samples of the DABA and its Schiff bases were weighed in the order of 1, 5, 10, 20 and 25 mg, respectively. Samples were diluted by 10 mL DMSO and then, 5 mL of 20% Tween 80 solution was added to increase the solubility. The solutions were diluted to maximum of 100 mL using sea water. Due to the turbidity problem, the study was restricted above 25 mg dilutions. Trials were conducted with 10 mL of sample solution with 10 larvae at open condition. Test vials with larvae were set aside for 24 h along with 25 W tungsten lamp focus. Dead larvae were counted after the maintenance and percentage of mortality was calculated. From the triplicated assay result, the regression graph were plotted between the log C and percentage of mortality. Lethal concentration for 50% of mortality (LC_{50}) was calculated from the equations. DMSO and Tween 80 mixture was used as a negative control and vincristine sulphate was used as positive control to validate the test method [16].

Antibacterial activity: The antibacterial activity of the synthesized compounds was measured using agar diffusion, by following the standards set by NCCLS [17]. Antimicrobial activity was tested using Muller-Hinton Agar (MHA) (HiMedia, Mumbai). Under aseptic conditions in the Biosafety chamber, 15 mL of MHA medium was distributed into pre-sterilized glass petri dishes to develop a 4 mm depth and injected with bacteria. The sterile discs of 6 mm were impregnated with 50 μL DMSO concentration of the compounds and dried them for 10-15 min. Using flamed forceps, the dry discs were gently pressed over MHA agar to ensure contact. To control for micro-organisms, amoxicillin (50 μg) (HiMedia, Mumbai) was used as a positive control and DMSO as a negative control. The test samples were evaluated against *K. pneumoniae*, *S. typhimurium*, *E. coli* and *P. mirabilis*. Discs were far enough apart to avoid reflections from petri dish edges and inhibition rings. Finally, the petri dishes were incubated at 35 ± 2 ºC for 24 h. After three trials, zone of inhibition diameters were determined in mm. The percentage of activity index was determined from the zone of inhibition using the following formula:

$$\text{Activity index (\%)} = \frac{\text{Zone of inhibition by the test compound}}{\text{Zone of inhibition by standard}} \times 100$$

Radical scavenging assay: DPPH is one of the stable and commercially available organic nitrogen radical. It has a maximum absorption of UV-visible at 515 nm. Upon reduction, the solution colour intensity decreases and the reaction growth is conveniently observed by a spectrophotometer. DPPH radical scavenging test was carried using the following procedure [18]. Absolute methanol (3.7 mL) in all test tubes were taken along with blank and then, 100 μL of absolute methanol was added to the blank. Subsequently, diluted (100-500 μg) test samples were added in prepared tubes. In each test tube ascorbic acid (100 μL) and DPPH (200 μL) were added and incubated at dark conditions for 30 min. Reaction was monitored at 515 nm for 30 min. Using concentration and antioxidant activity %, a linear regression graph determined the EC_{50} value.

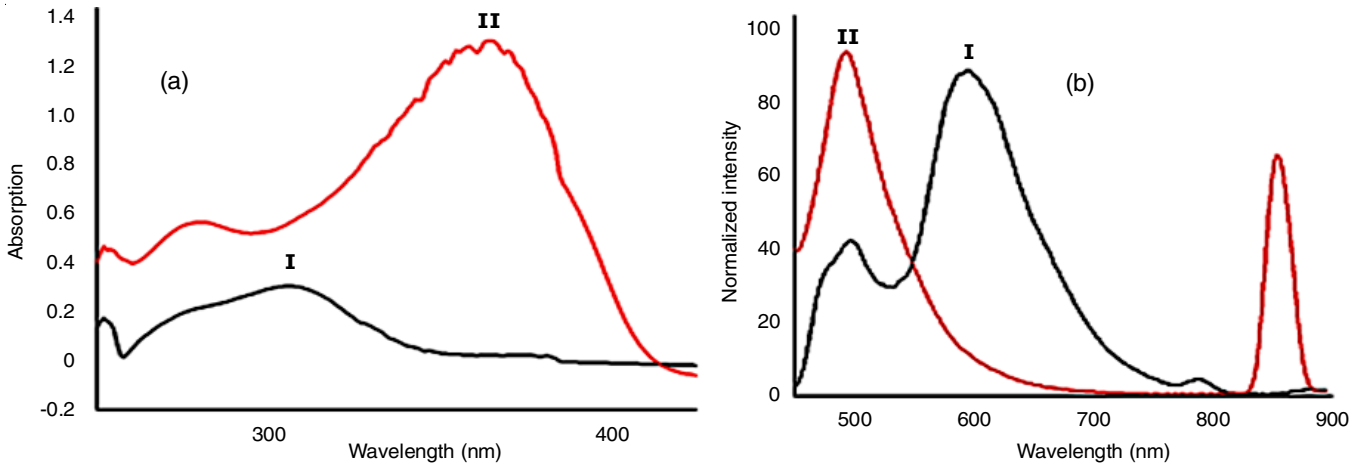

Fig. 1. (a) Experimental UV spectra of DABA based Schiff bases **I** and **II** in DMSO, (b) Fluorescence spectra of DABA based Schiff bases **I** and **II** in DMSO

$$\text{Antioxidant activity } (\%) = \frac{A_{blank} - A_{test}}{A_{blank}} \times 100$$

where abs. cont. = absorbance of DPPH at 517 nm as a control after 30 min of reaction.

RESULTS AND DISCUSSION

Two 4,4′-diamino benzanilide (DABA) based Schiff bases (**I** & **II**) for future drug discovery based on secondary amide group were prepared in methanol with good yield and characterized. Absorption spectra of Schiff bases (**I** & **II**) (Fig. 1a) displayed two main bands at 250-255 nm and 270-285 nm which are assigned to the $\pi \rightarrow \pi^*$ transitions of the aromatic rings [19]. An intramolecular charge transfer interaction can be linked to the longer wavelength band at 300-370 nm. Fig. 1b shows the fluorescence spectra of Schiff bases (**I** & **II**), which validate the Schiff bases functional groups. These results indicated that the derivatives structure affects emission λ_{max} and fluorescence quantum yield (φ). Schiff bases exposed strong fluorescence intensity. Due to hydrogen bonding in both Schiff bases, the stimulated molecule is more stable. Schiff bases (**I** & **II**) have also shown conjugation and substituent effects on emission intensity. Table-1 displays the computed values for UV absorption, fluorescence emission intensity and quantum yield. These quantum yield data validated the Schiff base functional group absorption and emission. The emission ratio relevant to transitions ($\pi \rightarrow \pi^*$, $n \rightarrow \pi^*$) confirmed the substituent effect on compounds through intensity changes. Both Schiff bases (**I** & **II**) fluoresced owing to the conjugation of connected aromatic rings in the benzamide molecules, however, aromatic ring functional groups affected intensity. A quantum yield below one indicates equivalence between absorption and emission. Better quantum yield (0.74) of Schiff base **II** than Schiff base **I** (0.61) verified the hydroxyl group impact on Schiff bases.

TABLE-1
UV ABSORPTION, FLUORESCENCE EMISSION AND QUANTUM YIELD OF THE SCHIFF BASES

Schiff base	UV λ (nm)	Fluorescence λ (nm)	Quantum yield Ø = Abs/Emis
I	306 (max) 277 ($n \rightarrow \pi^*$) 252 ($\pi \rightarrow \pi^*$)	497 (max) 596	0.61
II	365 (max) 278 ($n \rightarrow \pi^*$) 253 ($\pi \rightarrow \pi^*$)	493 (max) 855	0.74

Infrared studies: This research used IRPal-2 version software to evaluate the FT-IR spectra (Fig. 2) of the Schiff bases. The experimental infrared bands validate the presence of crucial functional groups such as azomethine, hydroxyl and amide. In experimental infrared spectroscopy, Schiff bases did not exhibit a strong peak at 3395 cm^{-1} corresponding to free amine. Concurrently, azomethine group stretching frequency new bands appeared in IR spectra at 1665 cm^{-1} and in the Schiff base **II** IR spectra at 1625 cm^{-1}. Both Schiff bases exhibit intramolecular hydrogen bonding due to *ortho*-hydroxyl group, which was confirmed by broad peak between 3500-3100 cm^{-1} [20]. Amide group of the molecules showed the peaks at 3060 and 3057 cm^{-1}, respectively.

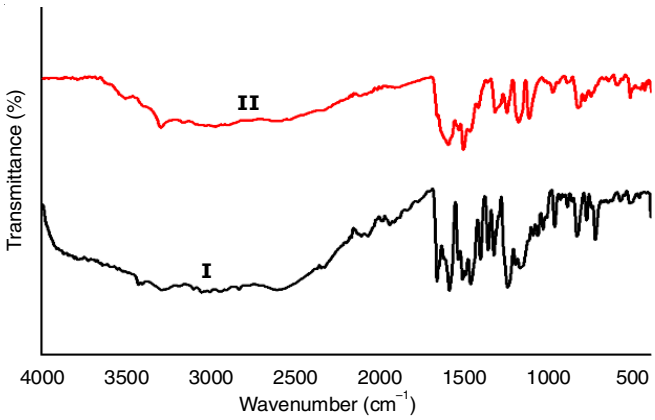

Fig. 2. Experimental FT-IR spectra of DABA based Schiff bases **I** and **II**

Schiff bases have shown the significant peaks for azomethine singlet proton at δ 12-13 ppm. Moreover, amide protons observed at δ 10.39-10.59 ppm and aromatic protons exist between δ 6.90 and 8.00 ppm. The above experimental protons

chemical shifts are concurrence with the testified values which are shown in Fig. 3a and 3b [21].

Spartan-14 DFT suit was used to predict various QSAR properties as shown in Table-2. The Lipinski five principles are a set of guidelines that are used to ascertain the medicinal potential of a molecule. In addition, the rule specifies that molecules that exhibit strong membrane permeability should have the following characteristics: a molecular weight of 500 or less, a number of hydrogen bond acceptors of 10 or fewer, a number of hydrogen bond donors of 5 or fewer and a total polar surface area of less than 140 $Å^2$. Both the molecules obeyed the Lipinski rules of five and carried for further biological studies. Additional, the HOMO and LUMO energy gap of Schiff bases (Figs. 4a-e) was calculated. The energy gap of Schiff base **I** (9.74 eV) is greater than Schiff base **II** (9.00 eV). The energy gap can be utilized to determine the reactivity and kinetic stability of the molecule. A smaller energy gap indicates the chemical reactivity and low kinetic stability since adding electrons to LUMO or removing electrons from HOMO is energetically encouraged [22]. The HOMO-LUMO energy separation classifies molecules by chemical hardness. Molecular electrostatic potential map (MEP) of the molecular structure shows the significant characteristics, hydrogen bond interactions and the link between the structure and its physico-chemical properties [23]. This study presents three-dimensional Schiff base molecular electrostatic potential (MEP) graphs (Figs. 4c & f). The negative spots are great for electrophilic attack symptoms, whereas the positive spots are ideal for nucleophilic attack. The potential increases from red to green to blue, with attraction strongest in blue and rejection strongest in red. In addition, the molecular polarity is inversely proportional to penetration, bioavailability for complexation and long half-life. Extension of the half-life of bioactive compounds increases their effectiveness in battling infections. The DFT analysis showed that its four hydroxyl groups gave it a greater potential than Schiff base **I**. The docking studies of Schiff base were based on DFT data and all the QSAR properties are fulfilled by the derived Schiff bases.

Ligand protein docking of the Schiff bases has been carried out against selected pathogens from *Escherichia coli* (Gram-negative bacteria) and *Staphylococcus aureus*, *Candida albicans* (Gram-positive bacteria). In order to provide context for the collected biological data and highlight potential relationships, we must consider Homo sapiens (α-amylase, cancer cell). The Schiff bases demonstrated a strong binding relationship by online docking methods when the test compounds were molecularly docked with the protein and enzyme receptors (Fig. 5). The online mcule server shown good docking scores for Schiff bases against *E. coli* cell division Zipa protein (1s1j), dehydrosqualene synthase enzyme of *S. aureuse* (2zcq), mRNA-capping enzyme subunit alpha of *C. albicans* (1p16), pancreatic α-amylase (1xcw) and breast cancer type 1 susceptibility protein (3k0k) targets and the free energy bindings of the Schiff bases are listed in

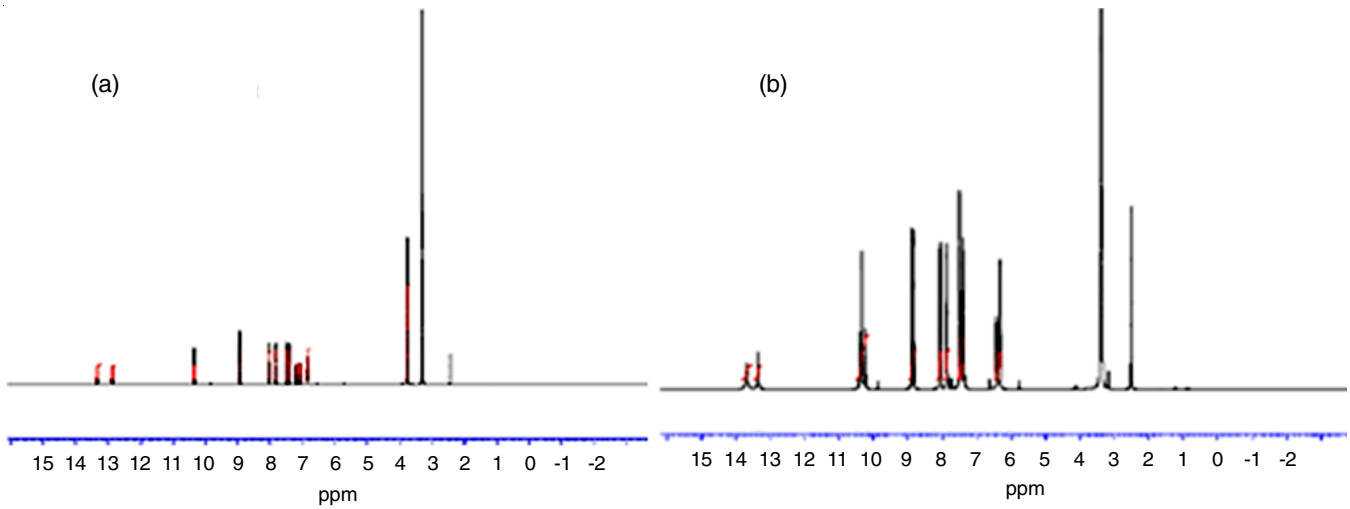

Fig. 3. ^{1}H NMR spectra of DABA based (a) Schiff base **I** and (b) Schiff base **II**

TABLE-2
QSAR PARAMETERS OF DABA BASED SCHIFF BASES

Properties	Schiff base **I**	Schiff base **II**	Parameters	Schiff base **I**	Schiff base **II**
Weight	467.481	485.503	HBA count	8	8
Area	473.97	483.77	Max epot	342.15	277.72
Min epot	-227.74	-251.86	HOMO (eV)	-7.78	-7.8
Min. localization ionic potential	51.52	54.38	LUMO (eV)	1.96	1.2
Log p	3.63	1.15	χ	2.91	3.3
HBD count	3	4	μ	-2.91	-3.3
Polar surface area	110.276	83.545	η	4.87	4.5
Polar area	174.21	171.04	S	0.102	0.11
Accepted polar area	125.83	129.32	ω	0.87	1.21
Polarizability	76.29	77.68	σ	0.20	0.22

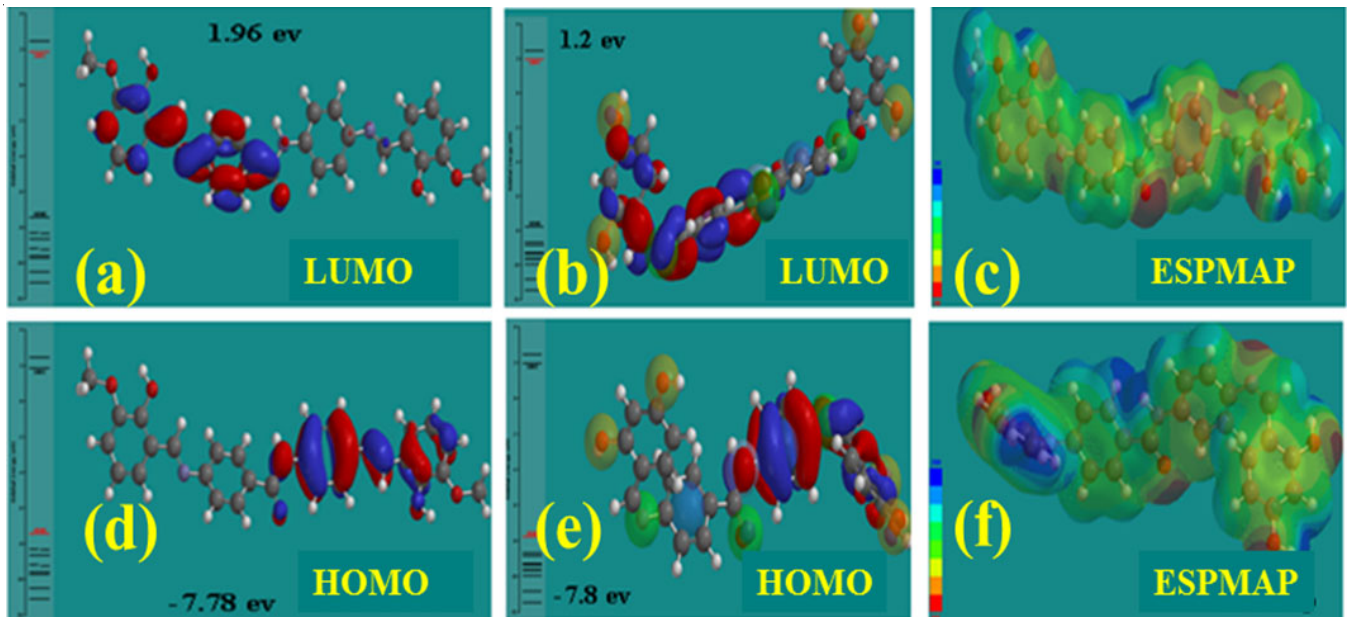

Fig. 4. (a) LUMO of DABA based Schiff base **I**, (b) LUMO of DABA based Schiff base **II**, (c) electrostatic potential map of DABA based Schiff base **I**, (d) HOMO of DABA based Schiff base **I**, (e) HOMO of DABA based Schiff base **II** and (f) electrostatic potential map of DABA based Schiff base **II**

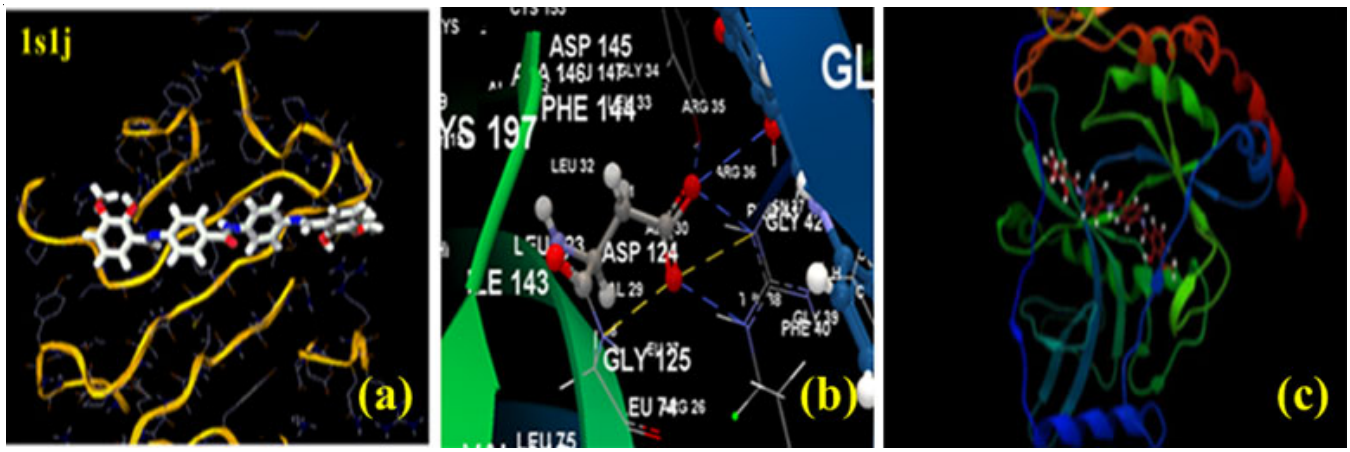

Fig. 5. (a) Mcule online docking images against the protein and enzyme targets of DABA based Schiff base **I**, (b) Active sites of the protein and (c) CLC docking image of DABA based Schiff base **I**

Table-3. Both the molecules are shown good binding affinity against the targets. The offline docking investigation was conducted to verify the online poses.

The results of the online docking were confirmed using the offline CLC drug discovery work bench-3 program. The common active sites such as glutamine, aspartame were selected

TABLE-3
MCULE ONLINE DOCKING SCORES AGAINST THE TARGETS

Target PDB id	Compd. ID	Pathogen/related biological study	Negative Docking score in kcal/mol				
			Pose1	Pose2	Pose3	Pose4	Best score
1s1j	Schiff base **I**	*E. coli*/Antibacterial (-ve)	7	6.9	6.7	6.4	7
	Schiff base **II**	*E. coli*/Antibacterial (-ve)	6.5	6.5	6.2	5.7	6.5
2zcq	Schiff base **I**	*Staphylococcus aureus*/Antibacterial (+ve)	10.9	10.8	10.6	9.4	10.9
	Schiff base **II**	*Staphylococcus aureus*/Antibacterial (+ve)	10.3	10.2	10.1	9.6	10.3
1p16	Schiff base **I**	*Candida albicans*/Antifungal	8.9	7.6	7.1	6.9	8.9
	Schiff base **II**	*Candida albicans*/Antifungal	8.7	8.6	7.2	7.1	8.7
1xcw	Schiff base **I**	Homo Sapiens/Antidiabetic	8.5	8.3	8.3	8.0	8.5
	Schiff base **II**	Homo Sapiens/Antidiabetic	10.2	10.0	9.9	9.4	10.2
3k0k	Schiff base **I**	Homo Sapiens/Antioxidant	7.2	6.7	6.5	6.4	7.2
	Schiff base **II**	Homo Sapiens/Antioxidant	6.9	6.3	6.1	5.9	6.9

TABLE-4
OFFLINE DOCKING SCORES AGAINST THE SPECIFIED TARGETS OF PROTEINS AND ENZYMES

Target PDB id	Compd. ID	Pathogen/Related biological study	Negative docking score in kcal/mol (active amino acid)	
1s1j	Schiff base **I**	*E. coli*/Antibacterial (-ve)	44.41 Glu50	48.06 (Asp91)
	Schiff base **II**	*E. coli*/Antibacterial (-ve)	44.35 Glu50	52.28 (Asp91)
2zcq	Schiff base **I**	*S.aureus*/Antibacterial (+ve)	50.25 (Asp124)	54.48 (Glu126)
	Schiff base **II**	*S.aureus*/Antibacterial (+ve)	59.35 (Asp124)	58.72 (Glu126)
1p16	Schiff base **I**	*Candida albicans*/Antifungal	57.88 (Glu162)	53.38 (Asp172)
	Schiff base **II**	*Candida albicans*/Antifungal	62.43 (Glu162)	65.58 (Asp172)
1xcw	Schiff base **I**	Homosapiens/Antidiabetic	59.9 (Asp147)	62.2 (Asp197)
	Schiff base **II**	Homosapiens/Antidiabetic	64.8 (Asp147)	66.8 (Asp197)
3k0k	Schiff base **I**	Homosapiens/Antioxidant	45.4 (Glu50)	47.3 (Asp91)
	Schiff base **II**	Homosapiens/Antioxidant	47.1 (Glu50)	43.9 (Asp91)

and docked offline CLC. Docking was carried out at active sites utilizing the setup binding site option in CLC-drug designing workbench-3. When tested against the target proteins, both Schiff bases demonstrated promising results (Table-4). The hydrophobic interaction between the protein and the essential amino acid components Asp (91, 147,197), Glu (2, 50) occurs at a radius of 13 Å. The docking scores of both Schiff bases (**I** & **II**) are ranged from -44 to -65 kcal/mol, clearly indicating the involvement of the amino acid residues.

Toxicity studies: The biological efficacy studies were based on the satisfactory theoretical results of QSAR and docking. The brine shrimp lethal test (BSLA) was used to determine the toxicity of the synthesized Schiff bases. When tested on brine Shrimp nauplii, the synthesized Schiff bases exhibited the considerable toxicity (Table-5). The LC_{50} values for the Schiff bases were evaluted from the regression graph (Fig. 6). The BSLA results showed that Schiff bases are safer than initial DABA dosages. Among the two Schiff bases, Schiff base **II** was linked with less adverse effects and had a more toxicity (307.97 µg/mL) than Schiff base **I** (281.86 µg/mL).

TABLE-5
THE BSLA LC_{50} VALUES OF SCHIFF BASES

Compounds	LC_{50} (µg/mL)
DABA % of mortality	214.86
Schiff base **I**	281.50
Schiff base **II**	307.97
DMSO + Tween 80	2718
Vincristin	0.583

Following the satisfactory analysis of the BSLA toxicity, an antimicrobial study was conducted for both Schiff bases containing secondary amide group. The antibacterial activity of Schiff bases was evaluated against selected bacterial strains using the well-diffusion method. Amoxicillin was used as a

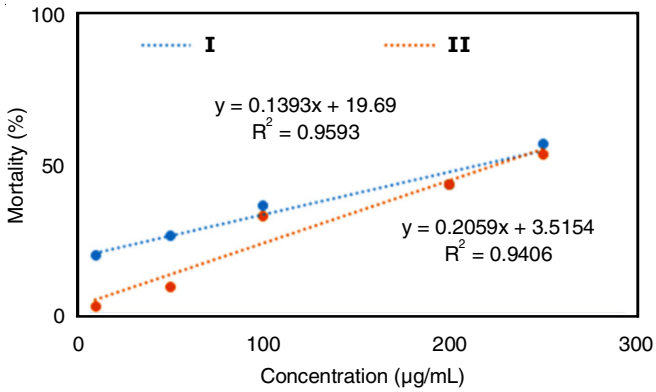

Fig. 6. Regression graph of BSL assay of DABA based Schiff bases **I** and **II**

reference to compare the activity. The inhibition zones were measured to determine the susceptibility of the Schiff bases, as reported in Table-6. The Schiff bases were evaluated against four Gram-negative bacteria using the agar well diffusion method. The results showed that Schiff base **I** had virtually the same zone of inhibition against the pathogens but Schiff base **II** has shown somehow better results against *A. baumannii* when compared to the amoxicillin standard. Similarly, Schiff base **II** revealed a nearly same zone of inhibition against *K. pneumoniae*. Both Schiff bases reported a percentage of activity index ranging from 42 to 99. The research revealed that both Schiff bases (**I** & **II**) have strong activity against some infections. The docking findings against Zipa (1s1j) cell division protein was consistent with the antibacterial effect of the synthesized Schiff bases.

Antioxidant activity: As the concentration of DABA based Schiff bases increased, so did their capacity to scavenge free radicals. The EC_{50} values of Schiff bases were found to be 303.27 and 222.9 µg/mL, respectively, according to the scavenging results, where Schiff base **II** > Schiff base **I**. All things considered, these results point to the fact that Schiff

TABLE-6
INHIBITION ZONE AND % OF ACTIVITY INDEX OF SCHIFF BASES

	Zone of inhibition (mm) for 150 µg (% of activity index)			
	E. coli	*K. pneumoniae*	*S. typhimurium*	*P. mirabilis*
Schiff base **I**	15 (53.6)	14 (77.8)	14 (44)	15 (42.9)
Schiff base **II**	19 (67.9)	16 (88.9)	15 (47)	17 (48.6)
DMSO-50 µL	–	–	–	–
Amoxicillin	28	18	32	35

bases significantly affect the free radicals. The data from this study showed that Schiff bases accomplish the docking result against cancer proteins and they are also free radical inhibitors, which means they may reduce free radical damage in the human body.

Conclusion

The synthesized Schiff bases (**I** & **II**) containing secondary amide group were extensively studied using ^{1}H NMR, fluorescence and ultraviolet (UV) spectroscopies. Moreover, the experimental as well as the theoretical biological investigations were also examined. The synthesized Schiff bases (**I** & **II**) were tested for toxicity and antibacterial activity against four Gram-positive pathogens. The experimental results were coincidental with the theoretical predictions. The DABA SBAs were docked online and offline using straightforward procedures in this study. The biological studies were successfully concluded by this research and the results align with theoretical approaches. The results for a 500 µg dilution of b were mild when compared to the *ortho*-vaniline Schiff base. The experimental results were in good agreement with the theoretical predictions. Beside its moderate antibacterial efficacy, antidiabetic activity and antioxidant activity, Schiff base b exhibited minimal toxicity (LC_{50} = 307.97 ± 2.8 µg/mL) and a exposed 281.50 ± 1.20 µg/mL, respectively. There has been an existence of activity concentrations within the LC_{50}. Because, the b has two *p*-OH bonds and *o*-OH groups, which are intermolecular hydrogen bonds. Results are moderate, nonetheless, because of the amide group and four aromatic rings.

ACKNOWLEDGEMENTS

Authors wish to thank Dr. R. Jayaprakash, Associate Professor, Department of Chemistry, School of Arts and Science, Vinayaka Mission's Chennai campus, Vinayaka Mission's Research Foundation (Deemed University). Further we are grateful to Royal bio lab, Velacherry, Chennai. (TN) provided the lab facility to study antidiabetic and antioxidant tendency of our molecules.

CONFLICT OF INTEREST

The authors declare that there is no conflict of interests regarding the publication of this article.

REFERENCES

1. M.D. Martínez, D.A. Riva, C. Garcia, F.J. Durán and G. Burton, *Molecules*, **25**, 789 (2020); https://doi.org/10.3390/molecules25040789
2. J. Drabik, K. Korasiak, J. Chrobak, J. Woch, N. Brzezniak, W. Barszcz, R. Kozdrach and J. Ilowska, *Molecules*, **29**, 122 (2024); https://doi.org/10.3390/molecules29010122
3. M. Kokot, M. Weiss, I. Zdovc, L. Senerovic, N. Radakovic, M. Anderluh, N. Minovski and M. Hrast, *Eur. J. Med. Chem.*, **250**, 115160 (2023); https://doi.org/10.1016/j.ejmech.2023.115160
4. I. Tsacheva, Z. Todorova, D. Momekova, G. Momekov and N. Koseva, *Pharmaceuticals*, **16**, 938 (2023); https://doi.org/10.3390/ph16070938
5. A. Gumus, V. Okumus and S. Gumus, *Turk. J. Chem.*, **44**, 1200 (2020); https://doi.org/10.3906/kim-2005-61
6. Y. Vaghasiya, R. Nair, M. Soni, S. Baluja and S. Shanda, *J. Serb. Chem. Soc.*, **69**, 991 (2004); https://doi.org/10.2298/JSC0412991V
7. N. Galiæ, Z. Cimerman and V. Tomišic, *Spectrochim. Acta A Mol. Biomol. Spectrosc.*, **71**, 1274 (2008); https://doi.org/10.1016/j.saa.2008.03.029
8. S.D. Gupta, I.G. Mazaira, M.D. Galigniana, C.V.S. Subrahmanyam, B. Revathi, N.L. Gowrishankar and N.M. Raghavendra, *Bioorg. Chem.*, **59**, 97 (2015); https://doi.org/10.1016/j.bioorg.2015.02.003
9. S. Desai, P.B. Desai and K.R. Desai, *Heterocycl. Commun.*, **5**, 385 (1999); https://doi.org/10.1515/HC.1999.5.4.385
10. P. Pullumbi, S. Lemeune, J.M. Barbe, A. Trichet and R. Guilard, *J. Mol. Struct. THEOCHEM*, **432**, 169 (1998); https://doi.org/10.1016/S0166-1280(97)00411-9
11. F. Sonmez, Z. Gunesli, B.Z. Kurt, I. Gazioglu, D. Avci and M. Kucukislamoglu, *Mol. Divers.*, **23**, 829 (2019); https://doi.org/10.1007/s11030-018-09910-7
12. T.A. Yousef, O.A. El-Gammal, S.F. Ahmed and G.M. Abu El-Reash, *Spectrochim. Acta A Mol. Biomol. Spectrosc.*, **135**, 690 (2015); https://doi.org/10.1016/j.saa.2014.07.015
13. M.N. Uddin and M.S. Rahman, *J. Appl. Sci. Proc. Eng*., **10**, 29 (2023); https://doi.org/10.33736/jaspe.5133.2023
14. M.S. Meenukutty, A.P. Mohan, V.G. Vidya and V.G. Viju Kumar, *Heliyon*, **8**, e09600 (2022); https://doi.org/10.1016/j.heliyon.2022.e09600
15. D.R. Ruebhart, I.E. Cock and G.R. Shaw, *Environ. Toxicol.*, **23**, 555 (2008); https://doi.org/10.1002/tox.20358
16. A.S. Apu, M.A. Muhit, S.M. Tareq, A.H. Pathan, A.T.M. Jamaluddin and M. Ahmed, *J. Young Pharm.*, **2**, 50 (2010); https://doi.org/10.4103/0975-1483.62213
17. N. Vijayakumar, V.K. Bhuvaneshwari, G.K. Ayyadurai, R. Jayaprakash, K. Gopinath, M. Nicoletti, S. Alarifi and M. Govindarajan, *Saudi J. Biol. Sci.*, **29**, 2270 (2022); https://doi.org/10.1016/j.sjbs.2021.11.065
18. H. Gökce, Y.B. Alpaslan, C.T. Zeyrek, E. Aðar, A. Güder, N. Özdemir and G. Alpaslan, *J. Mol. Struct.*, **1179**, 205 (2019); https://doi.org/10.1016/j.molstruc.2018.11.005
19. R.M. Issa, A.M. Khedr and H.F. Rizk, *Spectrochim. Acta A Mol. Biomol. Spectrosc.*, **62**, 621 (2005); https://doi.org/10.1016/j.saa.2005.01.026
20. S. Samshuddin, B. Narayana, B.K. Sarojini, M.T.H. Khan, H.S. Yathirajan, C.G.D. Raj and R. Raghavendra, *Med. Chem. Res.*, **21**, 2012 (2012); https://doi.org/10.1007/s00044-011-9735-9
21. P. Kavitha, M. Saritha and K. Laxma Reddy, *Spectrochim. Acta A Mol. Biomol. Spectrosc.*, **102**, 159 (2013); https://doi.org/10.1016/j.saa.2012.10.037
22. H.A.R. Pramanik, D. Das, P.C. Paul, P. Mondal and C.R. Bhattacharjee, *J. Mol. Struct.*, **1059**, 309 (2014); https://doi.org/10.1016/j.molstruc.2013.12.009
23. F. Luque, J. López and M. Orozco, *Theor. Chem. Acc.*, **103**, 343 (2000); https://doi.org/10.1007/s002149900013